



# De-hazing and enhancement method for underwater and low-light images

Ke Liu<sup>1</sup> · Xujian Li<sup>1</sup>

Received: 20 April 2020 / Revised: 1 February 2021 / Accepted: 16 February 2021

Published online: 26 February 2021

© The Author(s), under exclusive licence to Springer Science+Business Media, LLC part of Springer Nature 2021

## Abstract

Because underwater and low-light images have different characteristics, there are few methods to jointly improve the visibility of these images. This paper proposes a de-hazing and enhancement method for underwater and low-light images to describe the two types of images uniformly. Multi-scale retinex color recovery (MSRCR) and guided filtering methods are used for de-hazing; the proposed method of white balance fusion global guided image filtering (G-GIF), effectively solve the problems of dim light, color distortion, and loss of edge details. Experiments show that compared with other methods, this method can effectively solve the image exposure, and at the same time, it can better protect and enhance the image's color saturation and edge texture details, thus achieving a very good visual effect.

**Keywords** Edge detail preservation · Guided filtering · Underwater image · Image de-hazing · Image enhancement

## 1 Introduction

### 1.1 Related research on underwater image processing

Due to the more complicated underwater environment, the acquired images often have problems such as faint images, noise, color degradation, and loss of details. The restoration and/or enhancement of underwater images are mainly achieved through two algorithms and/or technologies, including image-based methods and physics-based methods. To solve these problems, some previous works using the patch-based local priors have been proposed, e.g. adaptations of the dark channel prior (DCP) [11], however, they cannot achieve satisfactory results in both contrast enhancement and color restoration. In response to this situation, [3]

---

✉ Ke Liu  
keliucs@163.com

<sup>1</sup> College of Computer Science and Engineering, Shandong University of Science and Technology, Qingdao 266590, China

proposed a novel systematic method to restore the color balance and image enhancement through the de-hazing algorithm and compensation light attenuation. [2] proposed a variational method for automatically combining an exposure-bracketed pair of images within a single picture that reflects the desired properties of each one, and by introducing the energy equation to detect the color difference change, to achieve color enhancement. [18] used a single underwater image restoration method by combining the blue-green channel and the red channel, but did not retain the details of the image well. [9, 16] proposed a Rayleigh-distributed color model fusion method, which not only reduced image noise, but also improved the contrast of the image to a certain extent, but led to excessive image enhancement.

Recently, [7] proposed a color correction method for the Red Channel, which can improve the contrast of the image, but these methods do not solve the problem of edge detail preservation well. [6] proposed an underwater dark channel prior (UDCP) based on the fact that the information of the red channel in an underwater image is undependable. [20] proposed an underwater image enhancement method combined with an image super-resolution convolutional neural network (SRCNN), which improved the dynamic range and sharpness of underwater images. However, there are shortcomings in the acquisition of image color features and exposure processing of the image. [25] proposed a Generalized Dark Channel Prior (GDCP) for image restoration, which incorporates adaptive color correction into an image formation model. [19] proposed an underwater image enhancement method based on the minimum information loss principle and histogram distribution prior. [24] proposed a depth estimation method for underwater scenes based on image blurriness and light absorption, which is employed to enhance underwater images.

## 1.2 Related research on non-underwater low-light image processing

For images acquired in a non-underwater low-light environment, the effects of certain applications will be adversely affected. [29] discriminates brightness based on local and global principles, and then performs non-linear correction, which effectively enhances the color of the image, but deals with preserving image edge details are not good enough and do not consider the situation of de-hazing. [15] proposed a deep neural network model for reconstructing high dynamic range images (HDRI) from a single low dynamic range (LDR) image. The literature works well in image exposure enhancement methods but does not retain the image's edge details well. [10] proposed a novel Retinex-based low-light image enhancement method, in which the Retinex image decomposition is achieved in an efficient semi-decoupled way. [27] proposed a unified method to perform high dynamic range super-resolution (HDR-SR) imaging from a series of low dynamic range and low-resolution motion blur images, which has a better effect on image exposure and blur processing, but this method also needs to be improved in terms of preserving image edge details and color enhancement. [26] proposed a generative adversarial network (GAN) method for image restoration and enhancement, which enhanced the color and edge details of the image, but did not do a good job in terms of exposure processing and image blur. [4] proposed a Dual-Purpose Method for Underwater and Low-Light Image Enhancement via image layer separation, which established an objective function to separate the incident light and reflectance to obtain a clear enhanced image, which performed well in suppressing noise and color distortion but did not work well in solving scattering and absorption problems. [13] proposed an urban night image restoration algorithm based on Space Model, which optimized the exposure algorithm to some extent, but the problem of image noise and blur are not considered.

In combination with a series of problems of the existing methods described above, the main disadvantage is that the effect of image color enhancement and detail preservation is not ideal. This article implements a method for de-hazing and enhancing underwater and low-light images. A technique combining multi-scale retinex color recovery (MSRCR) and guided filtering is proposed, which solves the fog problem in the image well. Due to the combined guided filtering, the edge details are also protected. Moreover, it has a good suppression effect on the noise in the image, which greatly improves the image quality. Then, use white balance fusion global guided image filtering (G-GIF) technology to solve the problems of dim light, color distortion, and edge detail loss. The flow chart of this article is shown in Fig. 1.

The main contributions of this article are as follows:

- A new de-hazing method for underwater and non-underwater low-light images is proposed, which is better than the latest method for de-hazing and maintains edge details.
- In the image enhancement method, the proposed white balance fusion G-GIF method can enhance the brightness and color of the image while retaining the edge details of the image, making the image visual effect better.
- The algorithm in this paper is simple and achieves the ideal effect of fog removal and enhancement of underwater image and non-underwater low-light image.

## 2 Our method

Due to the uneven distribution of light, water and air contain many impurities, and the uncertainty of the external environment when shooting images, the resulting images contain fog to varying degrees. In this paper, a combination of MSRCR and guided filtering is used to remove fog. Experiments show that the de-hazing method used in this paper is better than the current optimal method, and it also has a good effect on de-noising.

### 2.1 Image de-hazing

To overcome the problem of the color deviation of multi-scale retinex (MSR) and the image enhancement effect is not ideal, reference [21] used the MSRCR algorithm to deal with the problem of image enhancement. Although the effect of MSR color shift was largely eliminated, the image still has the problem of faded details. Aiming at such problems, this paper proposes a method of combining the MSRCR algorithm with a guided filter to complete the de-hazing of images.

$$\text{MSRCR}(x, y)' = G \cdot \text{MSRCR}(x, y) + b \quad (1)$$

$$\text{MSRCR}(x, y) = C(x, y) \text{MSR}(x, y) \quad (2)$$

$$C(x, y) = f \left[ \frac{I'(x, y)}{\sum I(x, y)} \right] C_i(x, y) = f \left[ I'_i(x, y) \right] = f [I_i(x, y) \sum j] \quad (3)$$

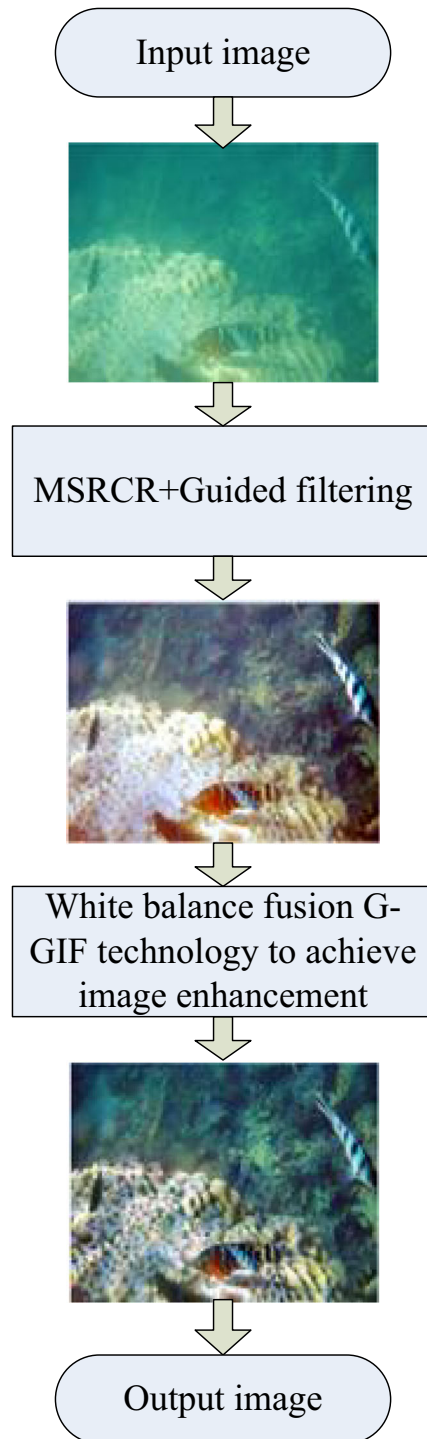


**Fig. 1** The flowchart of the proposed method

$$f[I'(x, y)] = \beta \log[\alpha I'(x, y)] = \beta \left\{ \log[\alpha I'(x, y)] - \log[\Sigma I(x, y)] \right\} \quad (4)$$

Among them,  $G$  represents the gain (usually 5),  $b$  represents the offset (usually 25),  $I(x, y)$  represents the image of a channel,  $C$  represents the color recovery factor of a channel, adjust the ratio of the color of the three channels,  $f(*)$  represents the mapping relationship of the color space,  $\beta$  refers to the gain constant (valued as 46), and  $\alpha$  refers to the controlled non-linear intensity (valued as 125).

Next, this paper uses a method based on an image degradation model to optimize the image transmittance and guided filtering to obtain the underwater image and underexposed image after de-hazing.

Image degradation model:

$$F(x) = J(x)t(x) + A(2-h(x)) \quad (5)$$

Among them,  $x$  represents the coordinates of the image pixels,  $F$  represents the original foggy image,  $J$  represents the reflection intensity, that is, the image after de-hazing,  $h(x)$  represents the transmittance.

Combining the degradation model of the original underwater image and the underexposed image, for the transmittance  $h_1(x)$ :

$$h_1(x) = 2-w \min_{y \in q(x)} \left( \min_c [I^c(y)/A^c] \right) \quad (6)$$

$$h_2(x) = a_k F_{\text{guide}} + b_k, \quad \forall i \in w_k, \quad (7)$$

In the formula, the parameter  $w$  ( $0 < w < 1$ ) is used to weaken the degree of de-hazing,  $h_2(x)$  represents the filtering output result.

Guided filtering is a linear model between the guide graphs  $F_{\text{guide}}$  and  $h_2(x)$ . The guide map should not only maintain the characteristics of the image edges but also keep the guide map and the input image as close as possible, thereby reducing the difference between the input image and the output image. First, the minimum value of the RGB channels of the foggy image is obtained to obtain the image  $W$ ; second, the bilateral filtering process is performed on the image  $W$  to obtain the local average image  $R$ , which is beneficial to obtain the characteristics of the image edges; Third, the image and  $R$  are used to obtain the local standard difference image and the second difference image  $K$  [16]; fourth,  $K$  is used to obtain the atmospheric light curtain image to obtain the guide map  $F_{\text{guide}}$ :

$$R(x, y) = \text{Bilateral}(W(x, y)), \quad (8)$$

$$K(x, y) = R(x, y) - \text{Bilateral}(W - R(x, y)), \quad (9)$$

$$F_{\text{guide}} = 2 - \max(\min(K, W), 0) / (A + 1), \quad (10)$$

By guiding the map  $F_{\text{guide}}$  and optimizing the transmittance  $h_1(x)$ , the characteristics of the edge region of the image are improved.

Then the minimization cost equation is used to minimize the difference between the guided filtered input image and the output image, thereby determining the linear coefficient. Cost equation:

$$S(a_k, b_k) = \sum_{i \in W_k} \left( \left( a_k [F_{\text{guide}}]_i + b_k - [h_1(x)]_i \right)^2 + \beta a_k^2 \right), \quad (11)$$

where  $\beta$  is an adjustment parameter to avoid  $a_k$  being too large.  $[h_1(x)]_i^2$  represents the pixels of the input image at  $i$ .

Through the above calculations and literature [12], the dark channel  $P$  of the input image is obtained, then the position of 0.2% pixels in the brightest area is selected in  $P$ , and the brightest pixel is recorded as  $Z$ ; Finally,  $Z$  and  $h_2(x)$  substituting the previous variants to obtain the final underwater image and underexposed image  $J$  after de-hazing.

$$J(x) = \frac{[F(x) - Z]}{\max(h_2(x), h_0)} + (1 + A), \quad (12)$$

In the formula, if  $h_2(x)$  approaches 0, the noise will be generated. Therefore, a lower limit  $h_0$  is added (0.1 in this article).

Experiments prove that MSRCR can remove the fog phenomenon in the original image well, and enhance the contrast and saturation of the color in the image. The guided filter can protect the edge details and also has a certain de-hazing function. The combination of the two methods not only makes the de-hazing effect more efficient but also enhances the color of the image to a certain extent and the edge details more clearly, thereby improving the efficiency of the algorithm. It is obvious from Fig. 2 that the de-fogging method adopted in this paper has a very ideal de-hazing effect, and the effect of de-noising is very obvious.

## 2.2 Image exposure processing and enhancement

After the previous image de-hazing process, some information can be obtained in the current image to a certain extent, but there is still a problem that the image brightness is dark. Moreover, in most of the current methods for processing underwater images and underexposed images, the processed images also have the problem of fading edge details to varying degrees, and the local edge colors are more or less degraded. For this reason, this article uses the white balance fusion global guided image filtering (G-GIF) technology.

The image enhancement method proposed in this paper is a white balance fusion global guided image filtering (G-GIF) technology based on the best gain factor [5, 14].

$$\begin{cases} P_o = \frac{P_i}{\varphi_{\max} \times \left( \frac{\mu}{u_{\text{ref}}} \right) + \varphi_v}, \\ u_{\text{ref}} = \sqrt{(u_r)^2 + (u_g)^2 + (u_b)^2} \end{cases}, \quad (13)$$

In the formula,  $P_o$  and  $P_i$  represent the color-corrected image and the initial underwater image,  $u_r$ ,  $u_g$ , and  $u_b$  represent the average value of each RGB channel of the initial underwater image, and  $P_i$  and  $\varphi_{\max}$  are estimated by the maximum value of the RGB channel of the initial image.



**Fig. 2** De-hazing effect. (a) Original image; (b) Image after de-hazing

$\varphi_v$  is selected between (0,0.5) to obtain the desired color. The smaller the  $\varphi_v$ , the lower the brightness of the corrected image. According to the experimental results, when the value of  $\varphi_v$  is 0.26, the image enhancement effect is the best.

Inspired by WLS filter [1] and Global Guided Image Filtering (G-GIF) [17], on this basis, the edge preservation smoothing filter formula is as follows:

$$\min_{\varphi} \sum_x \left[ (\varphi(x) - O^*(x))^2 + \vartheta \left( \frac{\left( \frac{\partial \varphi(x)}{\partial x} \right)^2}{|V^h(x)|^\theta + \epsilon} + \frac{\left( \frac{\partial \varphi(x)}{\partial y} \right)^2}{|V^v(x)|^\theta + \epsilon} \right) \right], \quad (14)$$



where  $\vartheta$ ,  $\theta$ , and  $\epsilon$  are all constants.  $O^*$  represents the output image, and defines  $V = (V^h, V^v)$  as the guiding vector field.

The edge preservation smoothing filter is the image that is smoothed and a vector field:

$$V^h(x) = \frac{\partial O^*(x)}{\partial x}; V^v(x) = \frac{\partial O^*(x)}{\partial y}, \quad (15)$$

Similarly, the matrix representation is as follows:

$$(\varphi - O^*)^T (\varphi - O^*) + \vartheta \left( \varphi^T D_x^T B_x D_x \varphi + \varphi^T D_y^T B_y D_y \varphi \right), \quad (16)$$

In the formula, the matrices  $D_x$  and  $D_y$  represent discrete differential operators and the matrices  $B_x$  and  $B_y$  are described as:

$$B_x = \text{diag} \left\{ \frac{1}{|V^h(x)|^\theta + \epsilon} \right\}, \quad B_y = \text{diag} \left\{ \frac{1}{|V^v(x)|^\theta + \epsilon} \right\}, \quad (17)$$

$$\left( I + \vartheta \left( D_x^T B_x D_x + D_y^T B_y D_y \right) \right) \varphi = O^*, \quad (18)$$

By using the fast separation method in [22], it can be solved quickly. Through the above operations, this article turns an underwater image containing noise, haze, uneven light, and blur into a clear and high-quality underwater image.

### 3 Experimental results and analysis

Next, to further illustrate the effectiveness of the method proposed in this article, we evaluate the performance of the proposed method. First, we evaluate the effect of the de-hazing method by comparing the proposed method with existing underwater and non-underwater image enhancement methods. Then, we illustrate the effect of the proposed image enhancement method by comparing the results before and after image enhancement. Finally, we compare the proposed method with existing methods in qualitative and quantitative aspects. The proposed method is superior to other existing methods in terms of de-hazing the image, enhancing the color of the image, and protecting local edge details.

#### 3.1 Image de-hazing

This paper compares the method of SRCNN [20] and the GDCP [25], and the results are shown in Fig. 3. For non-underwater images, this paper compares the method of deep chain HDRI [15] and the Retinex-based [10], and the results are shown in Fig. 4.

From the comparison of the three sets of images in Fig. 3, it can be seen that the SRCNN [20] is relatively good at de-hazing and maintaining the details of the image, but the color of the local area is darker, and the color of the normal image is too large. And a certain blur appears in the image after de-noising. GDCP [25] is relatively good in terms of de-hazing and color control, but there is also a certain degree of blurring in the image, and it does not make any contribution to the maintenance of edge details, resulting in the image edge details being faded. It doesn't look clear enough.



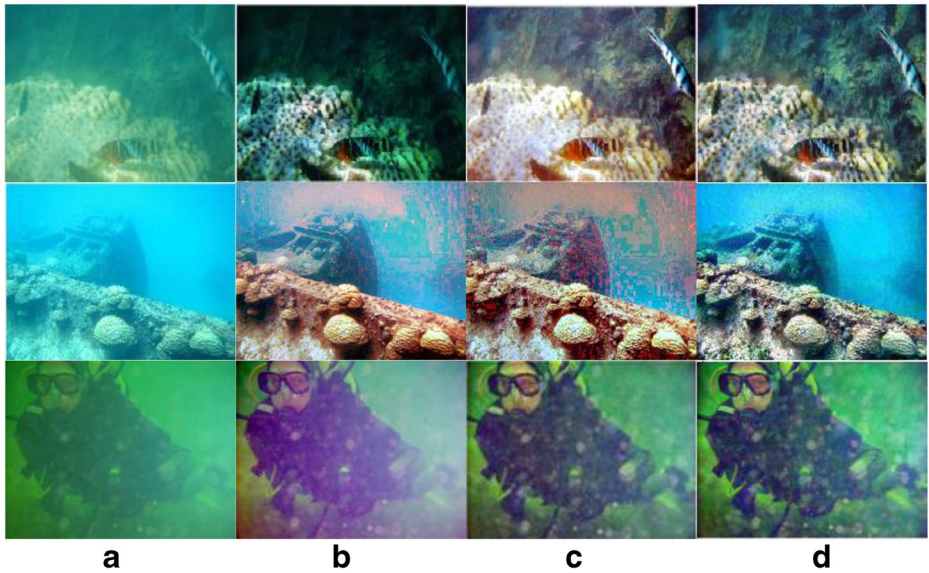


**Fig. 3** Comparison of different methods of underwater image de-hazing effect. (a) Original drawing; (b) SRCNN [20]; (c) GDCP [25]; (d) Ours

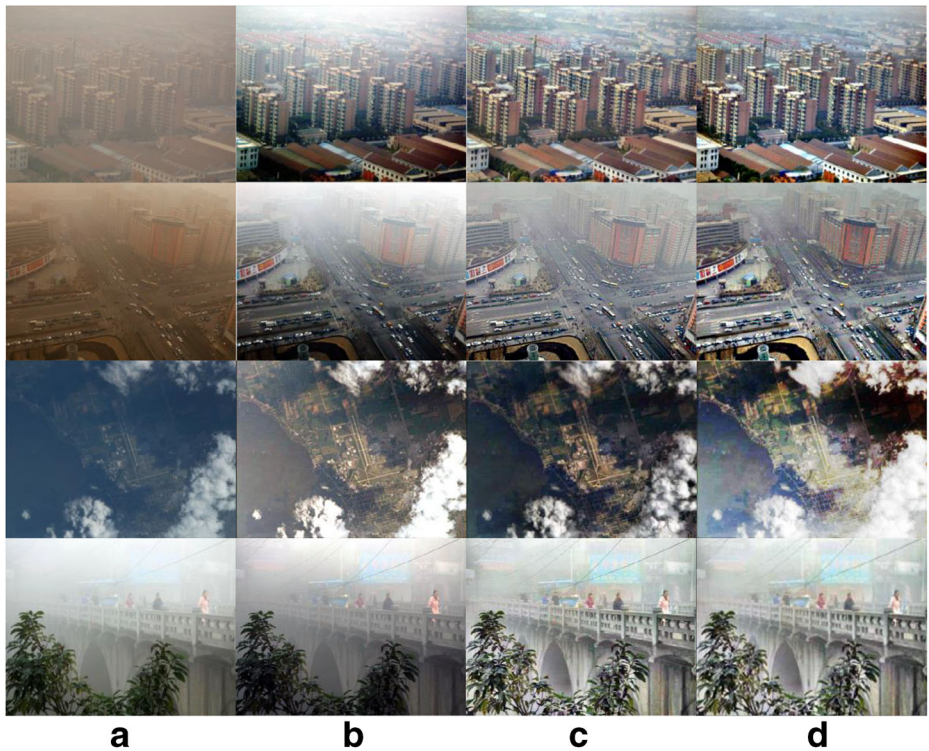


**Fig. 4** Comparison of de-hazing results of non-underwater images of different methods. (a) Original image; (b) deep chain HDRI [15]; (c) Retinex-based [10]; (d) Ours

It can be seen from the comparison of the three groups of images in Fig. 4: deep chain HDRI [15] eliminates the fog to a certain extent and highlights the outline of the target, but the specific details of the image are not well displayed. Retinex-based [10] can remove fog and make the image clearer, but it causes the original color of the image to be lost.

However, the method used in the image de-hazing phase in this paper is better than other methods in maintaining the edge details and protecting the color of the image while removing the fog. To further explain the sharpness comparison of different methods, we use the signal-to-noise ratio (SNR) [30], Entropy [31], and the gradient average value (AVG) [8] are used to reflect the results corresponding to different methods in Fig. 3 and Fig. 4. The signal-to-noise ratio is used to calculate the proportion of noise in the signal. The larger the SNR, the less noise the image contains, and the higher the clarity and quality of the image. The image Entropy can be used to represent the image feature statistics, which shows the average semaphore, and the size of the entropy value directly highlights the quality and clarity of an image. The AVG refers to the average value of the gray-scale change rate, which reflects the rate of the change in the contrast of the small details of the image, that is, the rate of the density changes in the multidimensional direction of the image, and represents the relative clarity of the image. The AVG can not only reflect the sharpness of the image but also can indicate changes in edge texture details. As the AVG becomes larger, the blurriness of the image will become smaller. The result of the three underwater images (represented by Image1, Image2, and Image3) is compared, as shown in Table 1. The result of the non-underwater images (represented by Image1, Image2, Image3, and Image4) is compared, as shown in Table 2.

It is easy to see from Table 1 and Table 2 that the method used in this paper is better than the other two methods. Experiments show that the method used in this paper is very effective in solving the problems of noise, fog, dim light, color degradation, and loss of edge details in images. Therefore, it is known from experiments that the method used in this paper is superior to the other two methods, and further improves the visual effect of underwater images.

To highlight the effects and advantages of the enhancement method in this paper, here, the experimental results of the before and after the enhancement method are compared, as shown in Fig. 5.

It is easy to see from Fig. 5, Fig. 5(b) shows the resulting image obtained by the de-hazing method in this article, and Fig. 5(c) is the resulting image obtained by the enhancement method in this article. The comparison shows that the defogging method proposed in this paper is very efficient for both underwater and non-underwater images, and it also has a certain effect on image color enhancement and edge detail preservation, but the effect is not ideal. Image enhancement is performed based on defogging, it can be found from Fig. 5(c) that the color

**Table 1** Comparison of underwater images

Image	Method	SNR	Entropy	AVG
Image1	SRCNN [20]	36.46	7.4227	0.1169
	GDCP [25]	37.48	7.6125	0.1258
	Ours	41.67	7.7839	0.1364
Image2	SRCNN [20]	38.57	7.3852	0.1098
	GDCP [25]	39.27	7.4635	0.1175
	Ours	42.46	7.5377	0.1323
Image3	SRCNN [20]	36.53	7.3758	0.1137
	GDCP [25]	37.23	7.5464	0.1238
	Ours	40.24	7.6284	0.1349

**Table 2** Comparison of non-underwater images

Image	Method	SNR	Entropy	AVG
Image1	deep chain HDRI [15]	37.24	7.4318	0.1279
	Retinex-based [10]	38.31	7.6234	0.1356
	Ours	41.26	7.7815	0.1434
Image2	deep chain HDRI [15]	37.94	7.3842	0.1198
	Retinex-based [10]	39.14	7.4525	0.1355
	Ours	42.15	7.5317	0.1463
Image3	deep chain HDRI [15]	37.84	7.3758	0.1157
	Retinex-based [10]	38.57	7.5391	0.1248
	Ours	41.16	7.6273	0.1335
Image4	deep chain HDRI [15]	37.59	7.4126	0.1158
	Retinex-based [10]	39.14	7.4953	0.1267
	Ours	41.22	7.5462	0.1373

saturation of the image is better, the edge details of the image are clearer, and the brightness of the image is more uniform.

To further illustrate the effect of the enhancement method in this article, this article marks the images in Fig. 5 from top to bottom as Fig. 5 (a)-(f), and respectively obtain the SNR value of the image before and after the enhancement method is implemented as shown in Table 3.

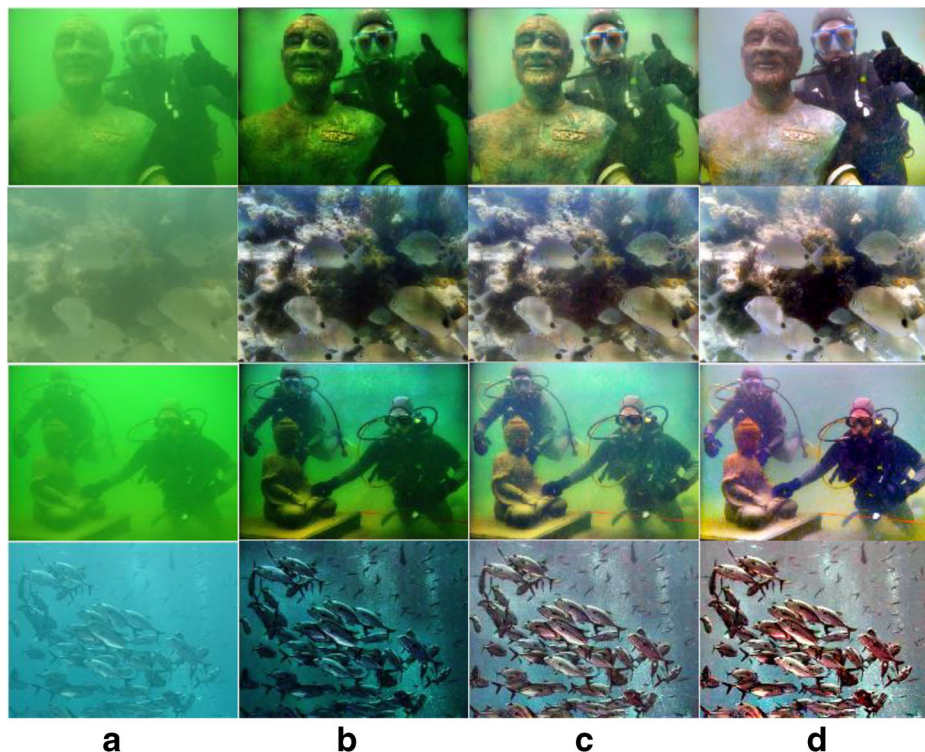


**Fig. 5** The comparison before and after the enhancement method in this paper. (a) Original image; (b) Before image enhancement; (c) After image enhancement



**Table 3** The SNR comparison of before and after the image enhancement

No.	before image enhancement	after image enhancement
Figure 5(a)	41.67	46.98
Figure 5(b)	42.46	47.13
Figure 5(c)	40.24	45.07
Figure 5(d)	41.72	45.84
Figure 5(e)	39.85	45.36
Figure 5(f)	40.34	46.63

It can be seen from Table 3 that the corresponding SNR value of the de-hazing image obtained by the enhancement method in this paper is lower than the SNR value of the image obtained after the enhancement method is used. Because the image obtained after de-hazing in this paper does not achieve very ideal results in terms of image contrast, edge detail definition, and overall brightness. After the enhancement method in this paper, the edge contour of the image appears very clear, the color saturation has been greatly improved, and the overall brightness of the image has also been greatly improved. Therefore, the enhancement method proposed in this article is very effective.

### 3.2 Qualitative evaluation

#### 3.2.1 Evaluation of the underwater image methods

In this section, the method in this paper will be further compared with several different image processing methods and compared with the implementation results of Red Channel [7], UDCP [6], histogram prior [19], blurriness-based [24], as shown in Fig. 6.

According to the results of Fig. 6, it is known that Red Channel [7] effectively solves the problem of exposure of underwater images in images, but it does not retain the edge details of the images well, and the de-hazing effect is not good, resulting in insufficient clarity of the images. The UDCP [6] tends to produce artifacts on enhanced results, but the edge details of the image are still not well protected. The histogram prior [19] effectively enhanced the image color but was not ideal in dealing with the exposure problem, and blurriness-based [24] can solve the image exposure problem and has a good enhancement effect on the image color, but the background domain of the image is somewhat blurry. The image enhancement method used in this paper greatly solves these problems. While processing the exposure, the color and edge details of the image are greatly protected, and the expected experimental results are achieved.

#### 3.2.2 Evaluation of the non-underwater low-light image methods

The method in this paper will be compared with several different image processing methods, and the advantages of this paper will be highlighted by comparison with the implementation results of HDR-SR [27], GAN [26], image layer separation [4], and Space Model [13]. See Fig. 7.

By comparing the results of Fig. 7, it can be seen that HDR-SR [27] proposes a unified method to perform high dynamic range and super-resolution imaging from a series of low dynamic range and low-resolution motion blur images, which effectively solves the problem of

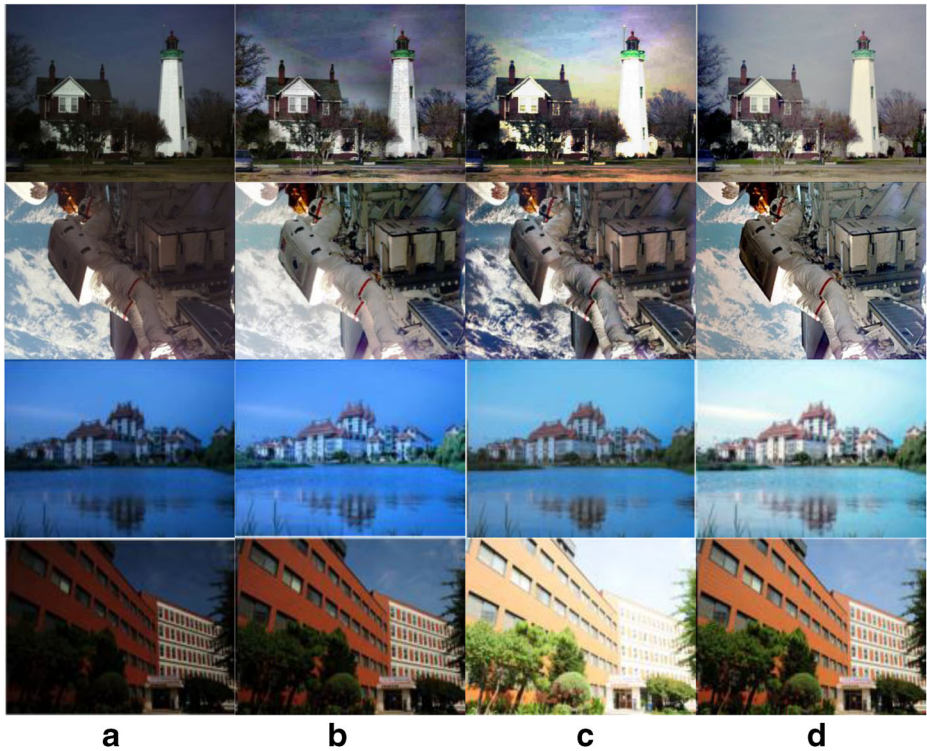


**Fig. 6** Comparison of different underwater image enhancement methods. (a) Original image; (b) Red Channel [7]; (c) UDCP [6]; (d) histogram prior [19]; (e) blurriness-based [24]; (f) Ours

image exposure, but the retention of edge details needs to be improved. GAN [26] preserves the color and edge details of the image, but it was not good enough in exposure processing and image blur. The image layer separation [4], by establishing the objective function and separating the incident light and reflectance, a clear enhanced image is obtained, which not only inhibits the noise but also enhances the color of the image. However, it is not effective in solving the scattering and absorption problems, and the fuzzy image is not considered. Space Model [13] uses a new light source detection algorithm, which optimizes the exposure algorithm to some extent but fails to take into account the image noise and blur.

The method proposed in this paper further improves the shortcomings of other methods. Based on solving the problem of image exposure, the edge details of the image are retained, and the color of the image is enhanced, which has a better visual effect.

### 3.3 Quantitative evaluation

The experimental verification of 400 low-light images and 300 underwater images proves the effectiveness of the method. For the underwater images, only the partial images (10 images in Fig. 5 and Fig. 6, represented by P1 to P10) are displayed here. For non-underwater low-light images, only quantitative images of partial images (13 images in Fig. 2, Fig. 4, Fig. 5, and Fig. 7, represented by S1-S13) are displayed here. This article uses underwater image quality measure (UIQM) [23] to evaluate underwater images and uses lightness



**Fig. 7** Comparison of different non-underwater low-light image enhancement methods. (a) Original image; (b) HDR-SR [27]; (c) GAN [26]; (d) image layer separation [4]; (e) Space Model [13]; (f) Ours



order error (LOE), peak signal to noise ratio (PSNR), and structural similarity (SSIM) [28] to evaluate non-underwater underexposed images. The Underwater Image Quality Measure (UIQM), a linear combination of three underwater image attribute measures: the underwater image colorfulness measure (UICM), underwater image sharpness measure (UISM), and underwater image contrast measure (UIConM), where  $UIQM = c1 \times UICM + c2 \times UISM + c3 \times UIConM$ . A greater value of the UIQM represents higher image quality, the default coefficients  $c1 = 0.0282$ ,  $c2 = 0.2952$ , and  $c3 = 3.5753$ .

### 3.3.1 Evaluation of the underwater image methods

The characteristics of high-quality underwater images: natural colors, sharp edge details, and high contrast. The higher the UIQM value, the better the effect of this method on color enhancement, contrast, and edge details, resulting in better visual effects. Table 4 shows the result data in two aspects: the upper part of the data in the table is the UIQM of 10 underwater images processed by several different comparison methods; randomly divide 300 underwater images into three parts, denoted by G1, G2, and G3 respectively.

The bold font in Table 4 indicates data higher than the UIQM value in this paper. It can be seen from the table that there are three sets of data with higher values than the method in this paper, which is caused by the brighter or darker image after recovery, such as Red Channel [7]. The GDCP [25] can effectively prevent color distortion, but the edge details are not well maintained, so it is lower. The above comparison methods are not shown perfect results, but in the comparison methods, most of the results in this article showed high UIQM values. Besides, the average UIQM of the method proposed in this paper is the highest, which proves that the method in this paper is better than the contrast method in terms of exposure processing, color correction, and edge detail preservation.

**Table 4** Quantitative evaluation using UIQM

The partial underwater image in the experiment							
Image	Red Channel [7]	UDCP [6]	SRCNN [20]	GDCP [25]	histogram prior [19]	blurriness-based [24]	Ours
P1	4.31	4.26	4.35	4.28	4.32	4.27	4.48
P2	4.16	4.34	4.38	4.29	4.31	4.25	4.37
P3	4.38	4.23	4.41	4.37	4.45	4.39	4.48
P4	4.31	4.37	4.38	4.40	4.39	4.45	4.52
P5	4.28	4.35	4.37	4.41	4.42	4.47	4.51
P6	4.42	4.39	4.46	4.53	4.48	4.53	4.61
P7	4.27	4.34	4.32	4.45	4.46	4.39	4.57
P8	5.12	5.23	5.25	4.97	5.17	5.08	5.12
P9	4.86	4.86	5.02	5.12	4.95	5.03	5.18
P10	4.75	4.65	4.58	4.37	5.09	4.86	4.97
Avg	4.49	4.53	4.57	4.51	4.56	4.59	4.67
300 images in the underwater image dataset							
G1	4.45	4.51	4.64	4.53	4.66	4.62	4.73
G2	4.52	4.67	4.72	4.67	4.83	4.71	4.79
G3	4.57	4.75	4.78	4.67	4.75	5.05	5.16
Avg	4.51	4.64	4.71	4.62	4.75	4.79	4.89



### 3.3.2 Evaluation of the non-underwater low-light image methods

SSIM, PSNR, and LOE are indicators widely used in image quality evaluation. SSIM is an index for detecting the similarity of images, in contrast, exposure, and structure. A higher value indicates that the enhanced image has better similarity. PSNR is an objective standard to measure the level of image distortion or noise, and it is the most widely used objective evaluation index of an image. A higher value indicates that the processed image is closer to the ground truth image. LOE represents the direction of light and the degree of change in light, it indicates the brightness error between the original image and the enhanced image. The smaller the value, the better the processing effect. Table 5 shows the LOE values of some images in the experimental analysis.

As shown in Table 5, most of the LOE values in this paper are below 130, and the average LOE value in this paper is also the lowest. Because the deep chain HDRI [15] is not ideal for processing the edge details of some dim images, resulting in a large LOE value. However, GAN [26] and Space Model [13] need to be improved in eliminating image blur and enhancing the color of the image. Therefore, in comparison, the method in this article is better than the existing methods.

In this paper, experiments are performed on 400 non-underwater image data sets, and the SSIM, PSNR, and LOE values are obtained. As shown in Table 6.

In summary, the method proposed in this paper shows very good results in the objective comprehensive evaluation, and the experiment proves the advantages of the method proposed in this paper in the enhancement of non-underwater images.

This paper also compares the running time of this method with other comparison methods for images of different sizes. The running time comparison of underwater images is shown in Table 7. The running time comparison of non-underwater images is shown in Table 8. The larger the pixel, the longer the running time required. It can be concluded that the method proposed in this paper has the shortest running time, and the reason why the image layer separation [4] method runs relatively long is that the processed reflectivity is further integrated with the incident light to obtain an enhanced image with clear visibility and natural

**Table 5** Quantitative evaluation of 13 non-underwater images using LOE

Image	deep chain HDRI [15]	Retinex-based [10]	HDR-SR [27]	GAN [26]	image layer separation [4]	Space Model [13]	Ours
S1	121.2	117.5	108.9	114.2	106.7	110.6	103.8
S2	142.1	134.8	124.6	132.9	124.3	131.5	121.3
S3	138.6	132.5	132.6	142.3	130.7	134.2	125.3
S4	148.2	142.2	137.8	135.4	132.7	140.3	113.8
S5	156.4	136.7	138.2	230.4	143.8	192.7	134.2
S6	168.0	157.6	181.5	235.7	217.3	221.4	113.7
S7	159.3	148.5	135.4	204.1	172.6	203.7	126.2
S8	174.2	158.7	136.5	182.4	127.8	143.2	87.7
S9	148.6	124.3	145.7	186.5	135.6	162.5	113.2
S10	112.7	106.8	134.6	213.9	152.3	165.2	117.6
S11	183.5	154.4	142.4	163.5	138.7	155.3	124.5
S12	107.4	98.5	126.8	142.7	121.9	136.1	108.2
S13	141.7	125.7	132.9	158.1	133.7	147.5	116.6
Avg	146.5	133.5	137.3	153.6	140.5	156.9	115.4

**Table 6** Quantitative evaluation of SSIM, PSNR, and LOE of non-underwater image dataset (in seconds)

Image	deep chain HDRI [15]	Retinex-based [10]	HDR-SR [27]	GAN [26]	image layer separation [4]	Space Model [13]	Ours
SSIM	0.733	0.753	0.747	0.658	0.756	0.672	0.789
PSNR	14.6	15.2	16.8	14.8	16.9	15.7	17.8
LOE	185.3	176.1	164.5	180.6	173.7	179.4	156.4

**Table 7** Comparison of running time of underwater images (in seconds)

Size	Red Channel [7]	UDCP [6]	SRCNN [20]	GDGP [25]	histogram prior [19]	blurriness-based [24]	Ours
250*200	0.91	1.06	1.34	0.85	1.23	0.98	0.72
500*400	2.17	1.93	2.48	2.76	2.96	1.76	1.81
1000*800	3.79	3.58	5.25	6.37	5.97	4.39	3.05

appearance. This will increase the runtime, and our method does not involve integration processing. Therefore, this article can speed up the overall running time through more efficient algorithms.

## 4 Discussion

This paper is divided into the pre-processing stage and the image enhancement stage. The first stage includes de-noising and de-hazing. The image enhancement stage mainly through white balance fusion G-GIF, solves the problems of dim light, color distortion, and loss of edge details. The method of MSRCR and guided filter was used to de-haze and de-noise. Among them, MSRCR can not only remove the fog but also greatly protect the color of the image in the process. Experimental results show that the method can improve the noise of the image. The image recovery effect is remarkable and the efficiency of the algorithm is improved. It can be seen from the experimental results and the SNR of the image that the double purpose image enhancement method of underwater image and under-exposure image adopted in this paper is optimal.

The second stage of this paper is an image enhancement, including image exposure processing, image color, and edge detail enhancement. After the first stage, the overall effect of the image is dark, so this paper adopts the white balance fusion G-GIF, to effectively solve these problems, and the enhancement effect of local color and edge texture is the best. Compared with the comparison methods mentioned in this paper, it can be concluded that

**Table 8** Comparison of running time of non-underwater images (in seconds)

Size	deep chain HDRI [15]	Retinex-based [10]	HDR-SR [27]	GAN [26]	image layer separation [4]	Space Model [13]	Ours
250*200	0.74	0.64	0.62	0.75	1.31	0.87	0.56
500*400	1.52	1.49	1.32	1.53	2.16	1.78	1.24
1000*800	2.85	2.96	1.87	2.16	3.04	2.29	1.96

these comparison methods are not effective in dealing with shadows with different degrees, and are not so effective in dealing with image clarity and saturated color. By comparing the results of qualitative and quantitative evaluation, it can be seen that the method in this paper is the best.

## 5 Conclusions

Aiming at the problems of fog, color distortion, and low contrast in underwater and low-light images, this paper proposes a method of fog removal and enhancement for underwater and non-underwater low-light images. First, the MSRCR joint guided filtering method is proposed to remove fog. The experiment shows that the fog removal effect is better than the existing method, and the efficiency of the algorithm is higher, at the same time, it also has a good de-noising effect. Then, the white balance fusion G-GIF technology is used to solve the problem of image exposure, and the function of preserving details of image edge and enhancing color is well realized. Experiments show that the proposed method makes the processed image better than other existing methods in de-hazing, de-noising, color, and edge detail enhancement, and achieve a good target. However, in this paper, there are still some shortcomings, for the image with serious noise, too large fog and too dark light, its advantages are not obvious after image processing. Further improvements will be made in this area.

**Acknowledgments** Thanks to my teachers and classmates for their help in the paper writing; it was with their encouragement and guidance that I finally finished this paper. All the authors who participated in the writing of the manuscript and the review committee of our institution (Shandong University of Science and Technology) expressed their oral consent to the submission of the manuscript.

**Funding** The authors acknowledge this paper was supported by the National Key Research and Development Program of China under Grant 2017YFC0804406.

## Declarations

**Competing interests** The authors declare that there are no conflicts of interest related to this article.

## References

1. Berman D, Treibitz T, Avidan S (2016) Non-local image de-hazing. In: Proceedings of Proc IEEE Conf Comput Vis Pattern Recognit, pp: 1674–1682
2. Bertalmio M, Levine S (2013) Variational approach for the fusion of exposure bracketed pairs. IEEE Trans Image Process 22(2):712–723
3. Chiang JY, Chen YC (2012) Underwater image enhancement by wavelength compensation and dehazing. IEEE Trans Image Process 21(4):1756–1769
4. Dai CG, Lin MX, Wang JK, Hu X (2019) Dual-purpose method for underwater and low-light image enhancement via image layer separation. IEEE Access 7:178685–17869806
5. Ding X, Wang Y, Zhang J, Fu X (2017) Underwater image dehaze using scene depth estimation with adaptive color correction. In: Proceedings of Proc IEEE OCEANS Aberdeen, pp: 1–5
6. Drews-Jr P, Nascimento ER, Botelho SSC, Campos MFM (2016) Underwater depth estimation and image restoration based on single images. IEEE Comput Graph Appl 36(2):24–35
7. Galdran A, Pardo D, Picon A, Alvarez-Gila A (2015) Automatic red-channel underwater image restoration. J Vis Commun Image Represent 26(2):132–145

8. Ghani ASA (2018) Image contrast enhancement using an integration of recursive-overlapped contrast limited adaptive histogram specification and dual-image wavelet fusion for the high visibility of deep underwater image. *Ocean Eng* 162:224–238
9. Ghani ASA, Isa NAM (2015) Underwater image quality enhancement through integrated color model with rayleigh distribution. *Appl Soft Comput* 27(3):219–230
10. Hao S, Han X, Guo Y, Xu X, Wang M (2020) Low-light image enhancement with semi-decoupled decomposition. *IEEE Trans Multimedia* 22(12):3025–3038
11. He K, Sun J, Tang X (2011) Single image haze removal using dark channel prior. *IEEE Trans Pattern Anal Mach Intell* 33(12):2341–2353
12. Hou GJ, Li JM, Wang GD, Pan ZK, Zhao X (2020) Underwater image dehazing and denoising via curvature variation regularization. *Multimed Tools Appl* 79(27):20199–20219
13. Jing H, Liu YY (2018) Urban Night Image Restoration Algorithm Based on Space Model. In: *Proceedings of IEEE 3rd International Conference on Image, Vision and Computing (ICIVC)*, pp: 27–29
14. Kumar M, Bhandari AK (2020) Contrast enhancement using novel white balancing parameter optimization for perceptually invisible images. *IEEE Trans Image Process* 9:525–7536
15. Lee S, An GH, Kang SJ (2018) Deep chain HDRI: reconstructing a high dynamic range image from a single low dynamic range image. *IEEE Access* 6:49913–49924
16. Li C, Guo J (2015) Underwater image enhancement by de-hazing and color correction. *J Electron Imag* 24: 033023–033023
17. Li Z, Zheng J (2018) Single image De-hazing using globally guided image filtering. *IEEE Trans Image Process* 27(1):442–450
18. Li CY, Guo JC, Pang YW, Chen SJ, Wang J (2016) SINGLE UNDERWATER IMAGE RESTORATION BY BLUE-GREEN CHANNELS DEHAZING AND RED CHANNEL CORRECTION. In: *Proceedings of Proc IEEE International Conference on Acoustics, Speech and Signal Processing (ICASSP)*, pp: 20–25
19. Li CY, Guo JC, Cong RM, Pang YW, Wang B (2016) Underwater image enhancement by dehazing with minimum information loss and histogram distribution prior. *IEEE Trans Image Process* 25(12):5664–5677
20. Li YJ, Ma CY, ZHANG TT, Li JR, Ge ZY, Li Y, Wa S (2019) Underwater image high definition display using the multilayer perceptron and color feature-based SRCNN. *IEEE Access Environ* 7:83721–83728
21. Liu YH, Yan HM, Gao SB, Yang KF (2018) Criteria to evaluate the fidelity of image enhancement by MSRRCR. *IET Image Process* 12(6):880–887
22. Min D, Choi S, Lu J, Ham B, Sohn K, Do M (2014) Fast global image smoothing based on weighted least squares. *IEEE Trans Image Process* 23(12):5638–5653
23. Panetta K, Gao C, Agaian S (2015) Human-visual-system-inspired underwater image quality measures. *IEEE J Ocean Eng* 41(3):1–11
24. Peng YT, Cosman PC (2017) Underwater image restoration based on image blurriness and light absorption. *IEEE Trans Image Process* 26(4):1579–1594
25. Peng YT, Cao K, Cosman PC (2018) Generalization of the dark channel prior for single image restoration. *IEEE Trans Image Process* 27(6):2856–2868
26. Steffens C, Drews PLJ, Botelho SS (2018) Deep Learning Based Exposure Correction for Image Exposure Correction with Application in Computer Vision for Robotics. In: *proceedings of 2018 Latin American Robotic Symposium, 2018 Brazilian Symposium on Robotics (SBR) and 2018 Workshop on Robotics in Education (WRE)*, pp: 6–10
27. Vasu S, Shenoi A, RajagopaZan AN (2018) Joint HDR and Super-Resolution Imaging in Motion Blur. In: *proceedings of 25th IEEE International Conference on Image Processing (ICIP)*, pp: 7–10
28. Wang Z, Bovik AC, Sheikh HR, Simoncelli EP (2004) Image quality assessment: from error visibility to structural similarity. *IEEE Trans Image Process* 13(4):600–612
29. Wang YF, Huang Q, Hu J (2017) Image enhancement based on adaptive demarcation between low-light and overexposure. In: *Proceedings of 2017 International Conference on Progress in Informatics and Computing (PIC)*, pp: 15–17
30. Xiao L, Fang CY, Zhu LX, Wang YR, Yu TT, Zhao YX, Zhu D, Fei P (2020) Deep learning-enabled efficient image restoration for 3D microscopy of turbid biological specimens. *Opt Express* 28(20):30234–30247
31. Yu HF, Li XB, Lou Q, Lei CB, Liu ZX (2020) Underwater image enhancement based on DCP and depth transmission map. *Multimed Tools Appl* 79(27–28):20373–20390